Development of Mechanical Yam Vibrator with Adjustable Frequency and Amplitude at Federal University of Agriculture, Abeokuta, Ogun Nigeria

Kifilideen L. Osanyinpeju[1*], Adewole A. Aderinlewo [1], Olawale U. Dairo [1], Olayide R. Adetunji [2], Emmanuel S.A. Ajisegiri [1]

1. *Agricultural and Bio-Resources Engineering Department, College of Engineering, Federal University of Agriculture Abeokuta, Ogun State, Nigeria*
2. *Mechanical Engineering Department, College of Engineering, Federal University of Agriculture Abeokuta, Ogun State, Nigeria*

***** *Corresponding Author* email address*: amkifilideenosanyinpeju@gmail.com, prof_4us@yahoo.com*
Phone number: 07063856386, 07083506769

Abstract

Overtime weight loss and sprouting loss and sprouting of yam tubers during storage had been creating issues among farmers and storage Engineers. Interaction of energy with matter has tendency of bringing change in the matter. To establish the effect of mechanical vibration on the physical properties of yam tubers and sprouts; this study therefore developed mechanical yam vibration with adjustable frequency and amplitude at Federal University of Agriculture, Abeokuta, Ogun Nigeria. A mechanical yam vibrator having adjustable frequencies and amplitudes was developed with vibrating chamber of capacity size of 670 mm × 570 mm × 180 mm which can contain four tubers of yam at a time. Preliminary test was conducted on the developed mechanical yam vibrator to determine the variation of the displacement of the developed mechanical vibrator using a vibrometer. The preliminary test conducted indicates that the maximum displacement of the developed mechanical yam vibrator using a cam size of 5 mm, 10 and 20 mm are 4.66 mm, 9.09 mm and 17.30 mm respectively at different levels of frequencies (low frequency (1 – 5 Hz), medium frequency (60 – 100 Hz) and high frequency (150 – 200 Hz). This proved that the developed mechanical yam vibration provide variation in displacement and frequency which would help in generating different levels of displacement and frequency for the yam tubers to be vibrated.

Keywords: Mechanical vibration, Frequency, Amplitude, Yam tubers, cam and follower, spring, electric motor.

Introduction

Emergence of new organism mostly results from collision and constructive interference between living and non-living. The constructive inference between the two parts results into cell division and multiplication which eventually results into new organisms. This cut across micro – organisms and multi – cellular organisms. No new species would even emerge without the collision and constructive inference of the parent objects, where at least one of the species must be living thing. Human, poultry, reptile, amphibian, plant kingdom existence, obey this ideology. This indicates that an isolated living thing which does not have collision and constructive inference with it environment or surrounding (living and non – living thing) cannot emerge a new organism. Yam is a living species organism which emerge new species by having interference with the biotic and abiotic factor of the surrounding (Onyenwoke and Simonyan, 2014; Abewoy, 2021). At some point, during its life time when the environment is not favourable for growth that is when there is destructive interference of the yam with the surrounding (Cheema, 2010). During this period there is no enough water in the soil for the survival of the yam. This condition is referred to as water stress. The yam tuber goes to dormant or inhibits in order to survive during this period (Kevers *et al.,* 2010). During favorable environmental condition that is when there is constructive interference of the yam with the surrounding growth is promoted and sprouting of the yam tuber begins (Wickham, 2019). Modification on when sprouting emerges and inhibition occurs during the life cycle of yam can be carried out by manipulating on how the environment (living and non – living factors) interacts with the yam species.

Vibration is a mechanical phenomenon whereby oscillations occur about an equilibrium point in a regular repeating pattern (Ekeocha, 2018). The mechanical vibration parameters are importance physical quantities in industries that are characterized by the physical quantities, frequency, amplitude and time (Lamancusa, 2002). The various ways of generating mechanical vibration are unbalance mass and cam and follower mechanisms. Nitinkmar *et al.* (2014) have designed an exciter machine for experimentation purpose and testing products at different frequencies which used unbalanced mass mechanism. The exciter consisted five mainly parts: base frame, drive system (motor), eccentric mass, spring and top plate. The exciter was mainly made of mild steel, except elements like disc attached to motor which was made of aluminum. The drive systems include a permanent magnet types DC motor with variable speed. The disc with eccentric mass was attached to motor at one end. To achieve different excitations, variable speed knob was attached to DC motor to control both speed and excitation. The drive system achieves a speed between 0 rpm to 1440 rpm. Their exciter simply uses an eccentric mass to provide forced vibration. A cam and follower mechanism vibrating exciter is a force generator that provides vibration or excitation source (Pawar *et al.,* 2016). Pawar *et al.,* (2016) design and fabricated a mechanical vibration exciter. The exciter generated uniaxial vibrations using cam and follower mechanism. It was designed to produce displacement through a given range of frequency. The machine can be mechanical (using electric motor), electro-hydraulic or electro – dynamic to power the cam and follower mechanism.

Brian and Brandon (2010) have designed a mechanical vibration exciter table for beam, round, rectangular and square plates and slip table vibrations for laboratory demonstration. The mechanical vibration shaker devices designed was based on cam follower (roller) design with a spring utilized to hold the follower on the cam at all times. They indicated that the stroke range for their work was 3.18 mm. However, it was also stated that for slip table application, it has the ability of providing a stroke of 70 mm. In order to determine the frequency at which the shaker was operating, a reflective photo-transistor and a frequency to voltage converter was used. A Hewlett Packard Dynamic Signal Analyzer and ICP Sensor Power Unit were used to capture the data from the accelerometer. The Digital Signal Analyzer was used to output the operating frequency of the shaker as well as acceleration. The frequency output allowed for proper calibration of the photo-transmitter. Their results show that cam and follower mechanism can be used for simple harmonic motion.

The Vibration excitation devices can be powered by one of the following: electromagnetic, mechanical, hydraulic, pneumatic, or even acoustical powered (Pawar *et al*., 2016). In general, the electromagnetic shakers are the only devices capable of producing higher frequencies up 15 kHz. Mechanical and hydraulic/pneumatic mechanisms are currently limited to lower frequencies as 200 Hz. The acoustical methods are limited by the amplifier producing the power and the frequency response range of the loudspeaker being used. The largest amplitudes are attainable with a hydraulic exciter with the mechanical producing maximum displacements although at very low frequencies. Usually, the electromagnetic shakers can only produce displacements not greater than one inch. Nitinkumar *et al.* (2014) reported that the frequency range of mechanical vibrator (using eccentric and connecting link, scotch yoke, cam and follower or rotating unbalance mass mechanism) falls between 0 – 200 Hz while maximum displacement achievable is 25 mm.

The primary key to increased tuber productivity and all-year-round availability of seed tubers rest in success at preventing the initiation of dormancy and/or the ability to drastically break the long dormant period in whole tubers (and cause instantly the appearance of a sprout on the surface of the tuber). The study would help to examine the sprouting response of yam tuber to vibration and ascertain their correlation to vibration environment. The scope of this research work entails designing, constructing and performance evaluation on a mechanical yam vibrator with varying frequency and amplitude and carrying out application of mechanical vibration on the control of sprouting.

For the purpose of this research work cam and follower mechanism was used for easy adjustment and variation of the frequency and amplitude of the vibration of the system. This study developed mechanical yam vibration with adjustable frequency and amplitude at Federal University of Agriculture, Abeokuta, Ogun Nigeria.

2.0 MATERIALS AND METHODS

2.1 Materials used for the construction of the mechanical vibrating table

The main components of the rigid mechanical yam tuber vibrator were vibrating container, spring (stiffness element), cam lobe (inertia elements), follower, variable speed electric motor (vibration exciter), chain and sprocket, shaft, and the frames. All the materials used for the construction were locally available. To establish the construction of mechanical vibrating table the machines and tools used were hacksaw, bench vice, drilling machine, welding machine, bench grinder, hand grinder, bending machine, lathe machine, Drill bit, scriber, drilling machine, measuring tape, punch, chisel, spanner, screw driver and plier.

2.2 Design of machine components

The machine components were designed as follows:

2.2.1 Design for the shaft on which the cam would be mounted on

The material selected for the design and construction of the shaft of the vibrating machine was alloy steel its high strength. The length of the shaft was determined based on the length of the frame of the vibrating machine. The length of the frame was designed as 600 mm. The length of the shaft was designed to be greater than this value. The length of the shaft was taken as 720 mm. The shaft of the vibrating machine would be subjected to bending moment and deflection due to the cam mounted along the longitudinal axis of the shaft of the vibrating machine. As a result of that, stresses were set up due to bending moment, torque and shearing force but the latter is usually unimportant, particularly as its maximum value occurs at the neutral axis where the bending stress is zero.

The shaft was designed for bending, deflection and shear failure to obtain its safe diameter. The shaft of the vibrating machine was subjected to torque due to the power to be transmitted to vibrating system and bending moment due to the reaction on the cam mounted on it. The length of the shaft of vibrating machine designed as 720 mm and the maximum weight of the cam mounted on the shaft was designed as 2.563 N. The cam was designed to be positioned at the middle of the length of the shaft.

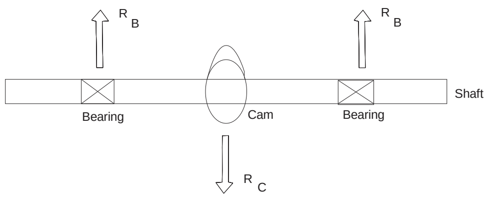

Figure 1 Freebody diagram of the shaft and the cam mounted on it

Both the bending stress σ and shearing stress τ respectively due to bending moment, M and torque, M_t have highest magnitudes σ_1 and τ_1 at the surface of the shaft or at point A. According to Ei *et al.* (2019) the maximum bending stress due to bending moment, σ_1 is given as:

$$\sigma_1 = \frac{32\,M}{\pi\,d^3} \tag{3}$$

Where,

$\sigma_1 -$ Maximum or greatest bending stress due to bending moment, N/m^2

$M -$ Maximum bending moment, Mm

$d -$ diameter of the shafτ_1 $-$t, m

Pederson (2010); Manikumar (2019) gave the maximum shear stress due to torsion as:

$$\tau_1 = \frac{16\,\mathrm{M}_t}{\pi\,d^3}, \tag{4}$$

Maximum or greatest shear stress due to torsion, N/m^2

$\mathrm{M}_t -$ Torque, Nm

$d -$ diameter of the shaft, m

The maximum principal stress for state of stress at point A, σ_{p1} is written by Khurmi and Gupta (2005) as

$$\sigma_{p1} = \frac{\sigma_1}{2} + \sqrt{\left(\frac{\sigma_1}{2}\right)^2 + {\tau_1}^2} \tag{5}$$

$$\sigma_{p1} = \frac{16\,M}{\pi\,d^3} + \sqrt{\left(\frac{16\,M}{\pi\,d^3}\right)^2 + \left(\frac{16\,\mathrm{M}_t}{\pi\,d^3}\right)^2} \tag{6}$$

$$\sigma_{p1} = \frac{16}{\pi\,d^3}\left(M + \sqrt{(M)^2 + (\mathrm{M}_t)^2}\right) \tag{7}$$

If we assume that a bending moment, M_e , acting alone would induce a bending stress, σ_{p1} at point A, then

$$\sigma_{p1} = \frac{32\ \mathrm{M}_{e\sigma_1}}{\pi\ d^3} \tag{8}$$

$$\mathrm{M}_e\ = \frac{1}{2}\left(M\ +\ \sqrt{(M)^{\ 2}\ + (\mathrm{M}_t)^2}\right) \tag{9}$$

$\mathrm{M}_e -$ the equivalent bending moment, Nm

Using equivalent bending moment for designing the shaft is same as using maximum normal stress theory of failure. The σ_b denote the permissible bending stress for the steel shaft, then

$$\sigma_b = \frac{32\ \mathrm{M}_e}{\pi\ d^3} \tag{10}$$

If we use maximum shearing stress theory then failure will occur when

$$\tau_{max} = \frac{16}{\pi\ d^3}\left(\sqrt{(M)^{\ 2}\ + (\mathrm{M}_t)^2}\right) \tag{11}$$

If we assume that a torque M_{te} acting along will cause same shearing stress as τ_{max}, then

$$M_{te}\ = \left(\sqrt{(M)^{\ 2}\ + (\mathrm{M}_t)^2}\right) \tag{12}$$

Where,

$M_{te}\ -$ the equivalent torque, Nm

The maximum bending moment, $M = \frac{Wl}{2}$ (13)

Where,

M – the maximum bending moment, Nm

W$-$ the weight of the cam mounted at the centre of the shaft, N

$l -$ the length of the shaft of the shaft of the vibrating machine, m

The length of the shaft of the vibrating machine was taken as 720 mm and the maximum weight of the cam mounted on it was determined as 2.563 N.

$$W\ = 2.563\ N,\quad l = 720\ mm = 0.72\ \mathrm{m} \tag{14}$$

The maximum bending moment, $M = \frac{2.563\ \times 0.72}{2} = 0.955\ Nm$ (15)

The designed power for the shaft of the vibrating machine was taken as 2 kW. The required speed of the electric motor required for the study 12, 000 rpm. Generally, mechanical exciters provide displacement up to 25 mm (Nitinkumar *et al.*, 2014). According to Savinkin *et al.* (2021) the electric power transmitted by the shaft of a machine is given as:

$$\mathrm{P} = \omega \times \mathrm{M}_t \tag{16}$$

$\omega = 2\pi N$ (17)

Where,

P = Electric power transmitted by the shaft, W

$\omega =$ angular velocity of the electric motor that power the shaft, rad/sec

$T =$torque transmitted by the shaft of the electric motor, Nm

N = frequency of the rotation of the electric motor, rev/sec (Hz)

P = 2 kW (18)

$N = 12,000$ revs/min = 12, 000 rev/ (60 sec) = 200 rev /sec

$\mathrm{M}_t = \frac{p}{2\pi N} = \frac{2000}{2\pi \times 200} = 1.59\ Nm$ (19)

Equivalent Bending moment was given as:

$\mathrm{M}_e = \frac{1}{2}\left(M + \sqrt{(M)^{2} + (\mathrm{M}_t)^2}\right) = \frac{1}{2}\left(0.995 + \sqrt{(0.995)^{2} + (1.59)^2}\right) = 1.4353\ Nm$ (20)

The equivalent bending moment, M_e will cause bending stress which was not allowed to exceed permissible value. Taking the permissible bending stress for steel shaft as 60 MN/m^2, then

$\sigma_b = \frac{32\ \mathrm{M}_e}{\pi\ d^3}$ (21)

Where,

$\sigma_b -$ the permissible or allowable bending stress for steel shaft

$\sigma_b = 60\ MN/m^2$, (22)

$\mathrm{M}_e = 1.4353\ Nm$ (23)

$60\ 000 = \frac{32 \times 1.4353}{\pi\ d^3}$ (24)

$d = 0.062\ m$ (25)

The used diameter of the shaft for its construction was 30 mm or 0.030 m. Since 0.062 m was not available in the market.

Testing for the safe level of the diameter of shaft 30 mm or 0.030 m we have

$\sigma_b = \frac{32\ \mathrm{M}_e}{\pi\ d^3} = \frac{32 \times 1.4353}{\pi\ (0.030)^3} = 541494.93\ N/m^2$ or $0.5419\ MN/m^2$ (26)

Since the bending stress (0.5419 MN/m^2) of the shaft on which the cam was mounted was less than the allowable or permissible bending stress (60 MN/m^2) for the span of 720 mm, therefore the design was acceptable. Indicating that diameter of 30 mm of the shaft of the vibrating machine was acceptable.

Equivalent torque was given as:

$$M_{te} = \left(\sqrt{(M)^{2} + (M_t)^2} \right) = \left(\sqrt{(0.995)^{2} + (1.59)^2} \right) = 1.8757\ Nm \qquad (27)$$

The equivalent torque will cause shearing stress which was not allowed to exceed permissible value. Taking the permissible or allowable shearing stress for solid shaft as 40 MN/m^2.

$$\tau_{allowable} = \frac{16M_{te}}{\pi\, d^3} \qquad (28)$$

Where,

$\tau_{allowable}$ – the permissible or allowable shearing stress, N/m^2

M_{te} – the equivalent torque, Nm

$$40\ 000 = \frac{16 \times 1.8757}{\pi\, d^3} \qquad (29)$$

$$d = 0.062\ m \qquad (30)$$

The used diameter of the shaft for its construction was 30 mm or 0.030 m. Since 0.062 m was not available in the market.

Testing for the safe level of the diameter of shaft 30 mm or 0.030 m we have

$$\tau = \frac{16M_{te}}{\pi\, d^3} \qquad (31)$$

$$\tau = \frac{16 \times 1.8757}{\pi\, d^3} \qquad (32)$$

$$\sigma_b = \frac{32 \times 1.8757}{\pi\, (0.030)^3} = 707644.42\ N/m^2 \text{ or } 0.7076\ MN/m^2 \qquad (33)$$

Since the calculated shearing stress (0.7076 MN/m^2) of the shaft on which the cam was mounted was less than the allowable or permissible shearing stress (40 MN/m^2) for the span of 720 mm, therefore the design was acceptable. Indicating that diameter of 30 mm of the shaft of the vibrating machine was acceptable.

Kilanko *et al.* (2020) suggested the modification of equivalent torque as:

$$M_{te} = \left(\sqrt{(K_m M)^{2} + (K_t M_t)^2} \right) \qquad (34)$$

From torsion equation, shear stress for shaft was given as the shaft diameter was given as

$$d^3 = \frac{16M_{te}}{\pi\, \tau} \qquad (35)$$

$$\tau = \frac{16}{\pi d^3} \left(\sqrt{(K_m M)^{2} + (K_t M_t)^2} \right) \qquad (36)$$

Where,

τ – shear stress for shaft, N/m^2

$K_m -$ combine shock and fatigue factor applied to bending moment

$\mathrm{K_t} -$ combine shock and fatigue factor applied to torsional moment

d – shaft diameter, m

$\mathrm{M}_t -$ torsional moment, Nm

$M -$ bending moment, Nm

The recommended values of K_m and $\mathrm{K_t}$ were 1.5 and 1.0 for steady load on a rotating shaft respectively. Testing the safe level of the selected available diameter (30 mm) found in the market for torsion we have

$\tau_{allowable} = 40\ MN/m^2$, $K_m = 1.5$, $\mathrm{K_t} = 1.0$, M = 0.995 Nm and $\mathrm{M}_t = 1.59\ Nm$ (37)

$\tau = \frac{16}{\pi\,(0.030)^3}\left(\sqrt{(1.5\ \times 0.995)\ ^2\ + (1.0\ \times 1.59)^2}\right) = 411366.52\ N/m2$ or $0.4114\ MN/m2$ (38)

Since the calculated shear stress (0.4114 MN/m^2) of the shaft on which the cam was mounted was less than the allowable or permissible shearing stress (40 MN/m^2) for the span of 720 mm, therefore the design was acceptable. Indicating that diameter of 30 mm of the shaft of the vibrating machine was acceptable.

The diameter of shaft used for the construction of the vibrating chamber was 30 mm.

Weight of the shaft of the vibrating chamber

The length and diameter of the shaft designed for were 720 mm and 30 mm respectively. From Okeke (2016); Anyakoha (2016) and Akusu *et al.* (2018) the weight of the shaft was determined as follow:

Weight of the shaft = $\rho V g = \rho A l g = \rho \frac{\pi d^2}{4} l g$ (39)

Where,

$\rho -$ density of the shaft

$V -$ Volume of the shaft

A – Cross-sectional area of the shaft

$d -$ diameter of the shaft

$l -$ length of the shaft

g – Acceleration due to gravity

From Engineering ToolBox (2008) the density of alloy steel was $8.05 \times\ 10^{3}$ kg / m^3. So,

Weight of the shaft $= \rho \frac{\pi d^2}{4} l g$ (40)

Weight of the shaft$= 8.05\ \times\ 10^{3}\ \times \frac{\pi (0.03)^2}{4} \times 0.72\ \times 10 = 40.97\ N$ (41)

Table 2 shows the design specification of the shaft on which the cam was mounted.

Table 2: Design specification of the shaft on which the cam was mounted

S/N	shaft parameters	Specification
1	Material selection	alloy steel
2	Length of the shaft	720 mm
3	Diameter of the shaft	30 mm
4	Weight of the shaft	40.97 N

2.2.2 Design of the cam

The material selected and used for the cam was high carbon steel so as to reduce wearing at the peripheral of the cam since the cam profile would be rubbing with the roller of the follower during operation. The base radius of the cam depends on the diameter of the shaft on which it would be mounted on. The designed diameter of the shaft on which the cam was mounted was 30 mm.

The base radius of the cam was 30 mm and used for the construction. The thickness of the cam was taken as 20 mm while 25.4 mm flat bar was rolled round the peripheral of the cam making the cam to have a thickness of 25.4 mm. Three cam sizes were used for the research work. Each cam size was developed based on the required amplitude of the vibration needed. The required amplitudes of vibration for the project were 5mm, 10 mm and 20 mm. These were achieved by making the maximum displacement from the base radius of the small, medium and large cams to their profiles to be 5mm, 10mm and 20 mm respectively.

The biggest size of the cam was used to determine the maximum weight of the cam excited on the shaft of the mechanical vibrator. To determine the mass of the biggest size of the cam, the cam profile was assumed to be a perfect hollow cylinder. According to Okeke (2016) and Anyakoha (2016)

Mass of cam = ρV (42)

Where,

$\rho -$ density of the cam

V$-$ Volume of the hollow cam

Volume of hollow cam = Volume of the solid cam − Volume of the cut part to form the hollow cam (43)

From Okeke (2016) and Anyakoha (2016)

Volume of hollow cam = $\frac{\pi D^2}{4}\ t - \frac{\pi d^2}{4}\ t$ (44)

Where,

D− the solid diameter of the cam

d −the diameter of the cut part to form the hollow cam

t – the thickness of the cam

Volume of hollow cam = $\frac{\pi D^2}{4}\ t - \frac{\pi d^2}{4}\ t = \frac{\pi t}{4}\ (D^2 - d^2)$ (45)

D = diameter of the base circle + maximum displacement from the base radius of the cams to its profiles

D = 30 mm $+ 20\ mm$ = 50 mm = 0.050 m (46)

d = diameter of the base circle = 30 mm = 0.030 m (47)

$t =$ 25.4 mm = 0.0254 m (48)

Volume of hollow cam = $\frac{\pi \times 0.0254}{4}\ (0.050^2 - 0.030^2) =\ 0.00003192\ m^3$ (49)

From Engineering ToolBox (2008) the density of high carbon steel was $8.03 \times\ 10^3$ kg / m^3.

Mass of cam = $\rho V =$ $8.03 \times\ 10^3\ \times 0.00003192$ = 0.2563 kg (50)

This mass of cam was used to design for the diameter of the shaft of the vibrator. The Table 3 presents the design specification of the cam while Plate 1 indicates the view of the fabricated 10 mm, 5 mm and 20 mm amplitude (maximum displacement) cycloid cam respectively used for the mechanical yam vibrator

Table 3: Design specification of the cam

S/N	Cam parameters	Specification
1	Material selection	High carbon steel
2	Radius of the base circle	30 mm
3	Mass of the (largest size) cam	0.2563 kg
4	Maximum displacement of the set of the cams from the base circle to their profile	5 mm – 20 mm
5	Thickness of the set of cams	25.4 Mm

2.2.3 Design of the follower

The selected material for the follower rod was galvanised steel due to high level of rigidity. In order to minimize cost and still achieve better result the thickness of the roller was made to be less than but closer to the thickness of the cam. The selected and used thickness of the roller of the follower for its construction was 20 mm. The diameter of the roller was taken as 10 mm. The diameter of the follower rod was taken as 20 mm.

The follower rod length was obtained taking into consideration the spring length. However, the follower rod length must be greater than the spring length. The free length of the spring designed for was 150 mm. The follower rod length was then taken as 490 mm.

From Okeke (2016) and Anyakoha (2016) the weight of the follower rod and the follower roller were determined as follow:

Weight of the follower rod = $\rho V g = \rho A h g = \rho \frac{\pi d^2}{4} h g$ (51)

Where,

$\rho -$ density of the follower rod

V$-$ Volume of the follower rod

A – Cross-sectional area of the follower rod

d $-$ diameter of the follower rod

h $-$ height of the follower rod

g – Acceleration due to gravity

From Engineering ToolBox (2008) the density of galvanised steel was 7.86×10^{3} kg / m^3. The diameter of the follower rod was taken as 20 mm (0.02 m) while the follower rod length (height) was then taken as 490 mm (0.49 m). These values were used for their construction.

So,

Weight of the follower rod $= \rho \frac{\pi d^2}{4} h g$ (52)

Weight of the follower rod $= 7.86 \times 10^{3} \times \frac{\pi (0.02)^2}{4} \times 0.49 \times 10 = 48.398\ N$ (53)

To determine the weight of follower roller the following procedure was used:

From Okeke (2016) and Anyakoha (2016)

The follower roller was assumed to be a solid cylinder

Weight of the follower roller = $\rho V g = \rho A t g = \rho \frac{\pi d^2}{4} t g$ (54)

Where,

$\rho -$ density of the follower roller

V$-$ Volume of the follower roller

A – Cross-sectional area of the follower roller

d $-$ diameter of the follower roller

h $-$ thickness of the follower roller

g – Acceleration due to gravity

From Engineering ToolBox (2008) the density of stainless steel was 8.00×10^3 kg / m^3. The selected and used thickness of the roller of the follower for its construction was 20 mm (0.02 m). The diameter of the roller was taken as 10 mm (0.1 m).

So,

Weight of the follower roller $= \rho \frac{\pi d^2}{4} t g$ (55)

Weight of the follower roller $= 8.00 \times 10^3 \times \frac{\pi (0.01)^2}{4} \times 0.02 \times 10 = 0.1257\ N$ (56)

Total weight of the follower rod and roller = Weight of the follower rod + Weight of the follower roller (57)

Total weight of the follower rod and roller = $48.398\ N + 0.1257\ N$ (58)

Total weight of the follower rod and roller = 48.5234 N (59)

Table 4 presents the design specification of the follower while Plate 2 indicates the view of the fabricated roller and follower of the mechanical yam vibrator.

Table 4: Design specification of the follower

S/N	Follower parameters	Specification
1	Material selection for follower rod	Galvanised steel
2	Material selection for follower roller	Stainless steel
3	Length of the follower rod	490 mm
4	Diameter of the follower rod	20 mm

5	Diameter of the follower roller	10 mm
6	Thickness of the follower roller	20 mm
7	Weight of the follower rod	48.398 N
8	Weight of the follower roller	0.1257 N


Plate 1 The view of the 10 mm, 5 mm and 20 mm amplitude (maximum displacement) cycloid cam respectively of the mechanical yam vibrator

Plate 2 The view of the roller and follower of the mechanical yam vibrator

2.2.4 Design of the frame of the vibrator

The selected material for the frame of the vibrator was two inches angle bar galvanized steel. The galvanized steel was selected due to its rigidity. The side length and breadth of frame were designed based on the length and breadth of the vibrating container. Since the length and breadth of vibrating container designed for were 600 mm and 570 mm respectively, therefore the length and breadth of the frame were taken as 600 mm and 570 mm respectively.

The parameter that determine the length of the frame leg were the follower rod length, spring length, diameter of the base circle of the cam and maximum displacement from the base radius of the cams to its profiles. The formula used to determine the length of the frame leg was given below:

The length of the frame length = length of the follower rod − length of the solid spring + diameter of the follower roller + diameter of the shaft + maximum displacement from the base radius of the cam to its profiles + the distance of the level of the shaft of the vibrator to the base of the frame (60)

It was noted that the level of the shaft of the vibrator from the base of the frame must be greater than the maximum displacement from the base radius of the biggest cam size to its profile so as to prevent the cam profile touching the ground when in operation. So, the selected the length of the level of the shaft of the vibrator to the base of the frame was 110 mm.

The length of the follower rod designed for was 290 mm, the length of the solid spring determined was 150 mm, the diameter of the follower roller was taken as 20 mm while the diameter of the shaft was taken as 30 mm. More so, the maximum displacement from the base radius of the biggest cam size to its profile designed for was 20 mm and the distance of the level of the shaft of the vibrator to the base of the frame is taken as 110 mm.

Therefore,

The length of the frame length = 490 mm − 150 mm + 20 mm + 30 mm + 20 mm + 110 mm = 520 mm (61)

The length of the frame used for the construction was 520 mm. The Table 5 shows the design specification of the frame of the mechanical vibrating table.

Table 5: Design specification of the frame

S/N	Frame parameters	Specification
1	Material selection	two inches angle bar galvanized steel
2	Length side of the frame	600 mm
3	Breadth side of the frame	570 mm
4	the distance of the level of the shaft of the vibrator to the base of the frame	110 mm
5	Length (height) of the frame leg	520

2.2.5. Design of the vibrating chamber

Design of the size of the yam tuber vibrating chamber

The size and capacity of the vibrating chamber was designed putting into consideration of the number of replicates for each treatment of the yam tuber. This implies that the size of the vibrating chamber must be able to contain the number of replicate for the experimental design. The chamber was of single layer.

For the experiment design and analysis for this study, the number of replicate was taken as 2 replicate per treatment. Since the weight of the yam tubers for the experimental design was of two factors (weight between 0.1 kg and 2.9 kg and weight 3.0 kg and 5.0 kg) and each was going to undergo the same treatment. Four yam tubers (two yam tubers of weight between 0.1 kg and 2.9 kg and two yam tubers of weight 3.0 kg and 5.0 kg) were loaded into the vibrating chamber at the same time and given the same treatment. Clearance between the yam tubers was also putting into consideration. So the number of yam tubers per vibration designed for was 4. Hard cut papers were used to demarcate the four yam tubers during the vibration to avoid rubbing and bruising of the yam tuber during vibration. Rubber was laid in the side both side and the base of vibrating chamber to allow soft rubbing of the yam tuber with the chamber so as to avoid bruising of the yam tuber during vibration. The Plate 3 indicates the view of the alignment of the yam tubers (weight between 0.1 kg and 2.9 kg and weight 3.0 kg and 5.0 kg) during the vibration.

Taking the shape of yam approximately cylindrical and having average diameter and length of 13 cm and 55 cm. Allowance was provided between yam tuber during design to allow for mobility during vibration as the yam tuber have more vibration impact under this condition than fixing it position during vibration.

Clearance was taken as 5 cm.

The length of the vibrating chamber = length of yam tuber + clearance = $55 + 5 = 60\ cm$ (62)

The breadth of the vibrating chamber = 4 × diameter of yam tuber + clearance = 4×13 + 5 = 57 cm (63)

The walls of the vibrating chamber were designed by putting into consideration the diameter (thickness) of the yam tuber. The height of the wall must be greater than diameter (thickness) of the yam tuber to prevent falling off of the yam tuber during vibration.

The height of the wall = the diameter (thickness) of the yam tuber + clearance (64)

The clearance was taken as 5 cm.

Therefore, the height of the each (front, back, left and right side) wall of the vibrating chamber = 13 + 5 = 18 cm (65)

The dimension (size) of the hollow cuboid vibrating chamber was $60\ cm\ \times 57\ cm \times 18\ cm$

The dimension (size) of the hollow cuboid vibrating chamber used for the construction of the chamber was $600\ mm\ \times 570\ mm \times 180\ mm$

The capacity (volume) of the hollow cuboid vibrating chamber = L×B×H= 0.60 m × 0.57 m × 0.18 m = 0.0616 m^3 (66)

Plate 3 The view showing the alignment of the yam tubers (weight between 0.1 kg and 2.9 kg and weight 3.0 kg and 5.0 kg) during the vibration

Thickness of the vibrating chamber

The follower rod was welded centrally beneath the vibrating chamber. Also, follower roller was welded at the end of the follower rod. The vibrating chamber was designed to bear the weight of follower rod and the follower roller without failing. The vibrating chamber was made from mild steel.

The total weight of the follower rod and follower roller designed for was 48.5234 N, so

The weight of the follower rod and follower roller was concentrated at the center of the vibrating chamber. For the design of the vibrating system, the vibrating chamber was supported by four springs of the same stiffness k, diameter d and length L. They were positioned at the bottom corner vertex of vibrating chamber. Let R_1 R_2 R_3 and R_4 be the reactions of the springs 1,2,3, and 4 respectively on the vibrating chamber. At the centre bottom base of the vibrating chamber the follower rod and follower roller of weight, W was welded. The Figure 2 presents the diagram of the vibrating chamber while Figure 3 shows free – body diagram of the vibrating chamber, the follower rod and follower roller.

Total upward force $= R + R_1 + R_2 + R_3 + R_4$ (67)

Since the springs are identical,

$R = R_1 = R_2 = R_3 = R_4$ (68)

Total upward force $= R + R + R + R = 4R$ (69)

R_i − the reaction of each of the spring on the corner end of the vibrating chamber, N

R − the total reaction of all the four spring, N

Total downward force $= W$ (70)

Where,

W = total weight of the follower rod and follower roller, N

Applying equilibrium equation

In x- direction, we have

$+\uparrow \sum F_x = 0,$ (71)

In y-direction, we have

$+\uparrow \sum F_y = 0,$ (72)

Total upward force – Total downward force $= 0$ (73)

$4R = W$ (74)

$R = \frac{W}{4}$ (75)

Where,

W = total weight of the follower rod and follower roller, N

R − the total reaction of all the four spring, N

Bending moment analysis,

$+\circlearrowright \sum M = 0,$ (76)

At $x = 0,\quad M = 0$ (77)

$x = x,$ M = 2R $\times x = \left(2 \times \frac{W}{4}\right) x = \frac{Wx}{2}$ (78)

$x = \frac{L}{2},$ M = $2\,R \times \frac{L}{2} = \left(2 \times \frac{W}{4}\right) \frac{L}{2} = \frac{WL}{4}$ (79)

$x = L,$ $M = (2\,R \times L) - \left(W \times \frac{L}{2}\right) = \left(2 \times \frac{W}{4} \times L\right) - \left(W \times \frac{L}{2}\right) = 0$ (80)

Therefore, the maximum bending moment = $\frac{Wl}{4}$ (81)

Where,

W = weight of the follower rod and follower roller

l = the length of the vibrating chamber

Weight of the follower rod and follower roller = 48.5234 N, Length of the vibrating chamber = 600 mm = 0.6 m

(82)

Maximum bending moment = M = $\frac{Wl}{4}$ (83)

Maximum bending moment = M = $\frac{48.5234 \times 0.6}{4} = 7.28$ Nm (84)

The figure 4 indicates the bending moment diagram of the vibration chamber. From flexure formula given by Socha *et al.* (2020),

The maximum bending stress of the base of the vibrating chamber = $\sigma_{max} = \frac{M}{S} = \frac{My}{I}$ (85)

Section modulus= S = $\frac{I}{y}$ (86)

y = $\frac{t}{2}$ (87)

Where,

σ = the maximum (permissible or allowable) bending stress, N/m^2

M = the maximum bending moment, Nm

S = Section modulus of the base of the vibrating chamber about the axis, m^3

y = the distance from the neutral axis to extreme edge of the cross section, m

I = the moment of inertia of the cross-sectional area about the neutral axis, m^4

t = the thickness of the vibrating the chamber, m

The maximum (permissible or allowable) bending stress for stainless steel, σ_{max} is 290 MN/m^2 (Childs, 2013).

M = 7.28 Nm, (88)

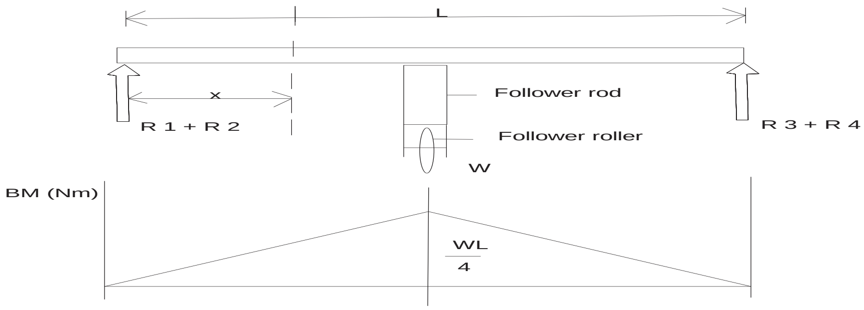

Figure 4 The bending moment diagram of the vibration chamber

y = $\frac{t}{2}$ (89)

I = $\frac{bt^3}{12}$ (90)

b = the width of the vibrating table = 570 mm = 0.57 m (91)

I =$\frac{bt^3}{12} = \frac{0.4t^3}{12}$ (92)

$\sigma = \frac{M}{S} = \frac{My}{I} = \frac{7.28\times\frac{t}{2}}{\frac{0.3t^3}{12}} = \frac{52.5\times t\times 12}{0.3\times t^3}$ (93)

Taking the thickness of the base of the vibrating chamber as 8 mm or 0.008 m, we have:

$\sigma = \frac{7.28\ \times 0.0204\times 12}{0.3\times 0.008\ ^3\times 2} = 5.8 \times 10^6$ N/m^2 or 5.8 MN/m^2 (94)

Since the bending stress (5.8 MN/m^2) of the base of the vibrating chamber due to the welding of the follower rod underneath the vibrating chamber was less than the allowable or permissible bending stress (290 MN/m^2) for the span of 0.60 m, therefore the design was acceptable. Indicating that thickness of 8 mm or 0.008 m of the base of the vibrating chamber was acceptable for the length of 0.60 m of the vibrating chamber.

For rectangular cross section,

Shear stress = $\tau = \frac{V\ Q}{Ib}$ (95)

I = $\frac{bt^3}{12}$, (96)

Q = A$\bar{y}$ = b$\times \frac{t}{2} \times \frac{1}{2} \times \frac{t}{2} = \frac{bt^2}{8}$ (97)

Where,

τ $-$ shear stress , N/m^2

V − maximum shear force, N

I − the moment of inertia of the cross-sectional area about the neutral axis, m^4

Q − first moment of the cross-sectional area, m^3

A − cross-sectional area of the base of vibrating chamber (m^2)

$\bar{y}$ − distance from neutral axis to centroid of area, m

b − width of the cross-sectional area, m

t − thickness of the vibrating chamber, m

Shear stress = $\tau = \frac{V\,Q}{Ib} = \frac{V \times \frac{1}{8} \times b \times t^2}{\frac{1}{12} \times b \times t^3 bt} = \frac{3\,\mathrm{V}}{2\,bt} = \frac{3\,\mathrm{V}}{2\,A}$ (98)

For the design of the vibrating system, the vibrating chamber was supported by four springs of the same stiffness k, diameter d and length L. they were positioned at the bottom corner vertex of vibrating chamber. Let R_1 R_2 R_3 and R_4 be the reactions of the springs 1,2,3, and 4 respectively on the vibrating chamber. At the centre bottom base of the vibrating chamber the follower rod of weight, W was welded.

Total upward force = $R + R_1 + R_2 + R_3 + R_4$ (99)

Since the springs are identical,

$R = R_1 = R_2 = R_3 = R_4$ (100)

Total upward force $= R + R + R + R = 4\,R$ (101)

R_i − the reaction of each of the spring on the corner end of the vibrating chamber, N

R − the total reaction of all the four spring, N

Total downward force $= W$

Where,

W = weight of the follower rod and follower roller, N

Applying equilibrium equation

In x- direction, we have

$+\uparrow \sum F_x = 0,$ (102)

In y-direction, we have

$+\uparrow \sum F_y = 0,$ (103)

Total upward force – Total downward force = 0 (104)

$$4\,R = W \tag{105}$$

$$R = \frac{W}{4} \tag{106}$$

Shearing force analysis,

At $x = 0$, $\quad S.F. =$ V = 2 R = $2 \times \frac{W}{4} = \frac{W}{2}$ (107)

$x = x$, $\quad S.F. =$ V = $2R = 2 \times \frac{W}{4} = \frac{W}{2}$ (108)

$x = \frac{L}{2}$, $\quad S.F. = V = 2R - W = \left(2 \times \frac{W}{4}\right) - W = \frac{W}{2} - W = -\frac{W}{2}$ (109)

$x = L$, $\quad S.F. = V = 2R - W + 2R = 4R - W = \left(4 \times \frac{W}{4}\right) - W = W - W = 0$ (110)

Where,

S.F. (V) – Shearing force

The maximum shearing force, V $= \frac{W}{2}$ (111)

Figure 5 gives the diagram of the vibrating chamber showing the forces acting on it while Figure 6 presents shearing force diagram of the vibrating chamber. Weight of the follower rod and follower roller = 48.5234 N, Length of the vibrating chamber = 600 mm = 0.6 m

Total weight of the follower rod and follower roller = W = 48.5234 N (112)

V = $\frac{W}{2} = \frac{48.5234}{2} = 24.2617\,N$ (113)

Shear stress = $\tau = \frac{V\,Q}{Ib}$ (114)

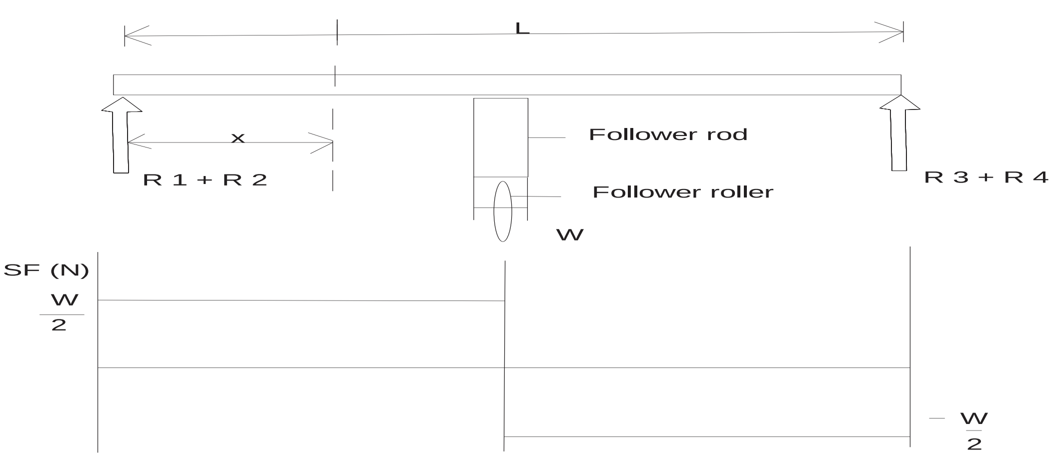

Figure 6 Shearing force diagram of the vibrating chamber

$I = \frac{bt^3}{12}$ (114)

$Q = A\bar{y} = b\times\frac{t}{2}\times\frac{1}{2}\times\frac{t}{2} = \frac{bt^2}{8}$ (116)

Shear stress $= \tau = \frac{V\,Q}{Ib} = \frac{V\times\frac{1}{8}\times b\times t^2}{\frac{1}{12}\times b\times t^4 b} = \frac{3\text{ V}}{2\,bt} = \frac{3\text{ V}}{2\,A}$ (117)

A = cross-sectional area of the base of vibrating chamber = bt (118)

b = the width of the vibrating table = 570 mm = 0.57 m (119)

A = 0.3 t (120)

The permissible or allowable shear stress for steel is 40 MN/m^2

Shear stress $= \tau = \frac{3\times 25.2617}{2\times 0.3\times t}$ (121)

Taking the thickness of the base of the vibrating chamber as 8 mm or 0.008 m, we have;

Shear stress $= \tau = \frac{3\times 25.2617}{2\times 0.3\times 0.008} = 15788.56\text{ N/m2 or }15.79\text{ kN/m2}$ (122)

Since the shear stress (15.79 kN/m^2) at the base of the vibrating chamber due to the welding of the follower rod and follower roller underneath the vibrating chamber was less than the allowable or permissible shear stress (40 MN/m^2) for the span of 0.6 m, therefore the design is acceptable. Indicating that thickness of 8 mm or 0.008 m of the base of the vibrating chamber was acceptable for the length of 0.6 m of the vibrating chamber and welded weight of the follower rod with follower roller as 48.5234 N.

Total weight of the vibrating chamber

Weight of the front and back walls of the vibrating chamber, W_{FB}

Volume of the front wall $= (L\times H\times t)$ (123)

Where,

L= 0.60 m, H= 0.18 m and $t = 0.008$ m (124)

Volume of the front wall $= 0.60\times 0.18\times\times 0.008$ (125)

Volume of the front wall $= 0.00086\ m^3$ (126)

Weight of the front wall $= \rho V g$ (127)

Where,

$\rho -$ density of the material used in the construction of the front wall, kg/m^3

V $- volume\ of\ the\ front\ wall,\ m^3$

g – acceleration due to gravity, m/s^2

The material used for the construction of the walls of the vibrating chamber was mild steel. From Engineering ToolBox (2008) the density of mild steel was 7.85 × 10^3 kg / m^3.

Therefore, the weight of the front wall $= \rho V g = 7850 \times 0.00086 \times 10 = 67.51\,N$ (128)

Weight of the front and back walls of the vibrating chamber $= 2 \times$ weight of the front wall$= 2 \times 67.51$ (129)

Weight of the front and back walls of the vibrating chamber $= 135.02\,N$ (130)

Weight of the left side and right walls of the vibrating chamber, W_{LR}

Volume of the left wall $= (B \times H \times t)$ (131)

Where,

B= 0.57 m, H= 0.18 m and $t = 0.008$ m (132)

Volume of the left wall $= 0.57 \times 0.18 \times 0.008 = 0.00082\,m^3$ (133)

Weight of the left wall $= \rho V g$ (134)

Where,

$\rho -$ density of the material used in the construction of the left wall, kg/m^3

V $- volume\ of\ the\ left\ wall,\ m^3$

g – acceleration due to gravity, m/s^2

The material used for the construction of the walls of the vibrating chamber was mild steel. From Engineering ToolBox (2008) the density of mild steel was 7.85 × 10^3 kg / m^3.

Therefore, the weight of the left wall $= \rho V g = 7850 \times 0.00082 \times 10 = 64.37\,N$ (135)

Weight of the left side and right walls of the vibrating chamber $= 2 \times$ weight of the left wall$= 2 \times 64.37$ (136)

Weight of the left side and right walls of the vibrating chamber $= 128.74\,N$ (137)

Weight of the bottom walls of the vibrating chamber, W_B

Volume of the bottom wall $= (L \times B \times t)$ (138)

Where,

L= 0.60 m, B= 0.57 m and $t = 0.008$ m (139)

Volume of the bottom wall $= 0.60 \times 0.57 \times 0.008 = 0.0027\,m^3$ (140)

Weight of the bottom wall $= \rho V g$ (141)

Where,

$\rho -$ density of the material used in the construction of the bottom wall, kg/m^3

V $- volume\ of\ the\ bottom\ wall,\ m^3$

g – acceleration due to gravity, m/s^2

The material used for the construction of the walls of the vibrating chamber was mild steel. From Engineering ToolBox (2008) the density of mild steel was 7.85×10^3 kg / m^3.

Therefore, the weight of the bottom wall $= \rho V g = 7850 \times 0.0027 \times 10 = 211.95\ N$ (142)

Total weight of the vibrating chamber $= W_{FB} + W_{LR} + W_B$ (143)

Weight of the front and back walls of the vibrating chamber, N

Weight of the left side and right walls of the vibrating chamber, N

Weight of the bottom walls of the vibrating chamber, N

Total weight of the vibrating chamber $= W_{FB} + W_{LR} + W_B$ (144)

$W_{FB} = 135.02\ N$, $W_{LR} = 128.74\ N$ and $W_B = 211.95\ N$ (145)

Total weight of the vibrating chamber $= 135.02\ N + 128.74\ N + 211.95 = 475.71\ N$ (146)

The Table 6 shows the design specification of the vibrating chamber.

Table 6. Design specification of the vibrating chamber

S/N	Vibrating chamber parameters	Specification
1	Material selection	Mild steel
2	Dimension	600 mm $\times$ 570 $mm \times$ 180 mm
3	Thickness of the walls and base of chamber	8 mm
4	Weight of the vibrating chamber	$475.71\ N$
5	Capacity	4 yam tubers
6	Method of joining of parts	Welding

2.2.6 Design of the helical spring

The spring used for the project was cylindrical helical spring made from chromium vanadium steel. The design of the spring was carried out by considering the weight of the vibrating chamber, weight of follower rod and follower roller. The four springs used helped in the suspension of the vibration chamber. The four springs were positioned at the bottom corner edges of the base of the vibrating chamber. The first priority of the suspension design for the suspender (springs) was for the four springs to be used to carry (support) and transmit the weight of the vibrating camber without failing. The following analyses were carried out for the purpose of making a reasonable selection of helical spring that will do the required job.

At equilibrium position the axial loads acting on springs 1 – 4 are P1, P2, P3 and P4 respectively. The axial load on each spring was assumed to be the same. The axial load on each spring was as result of weight of the vibrating chamber (W_C), weight of the follower rod (W_d) and the weight of follower roller (W_l). The Figure 7 presents the freebody diagram of the vibrating chamber and the spring.

Applying equilibrium equation

In x- direction, we have

$$+\uparrow \sum F_x = 0, \quad (147)$$

In y-direction, we have

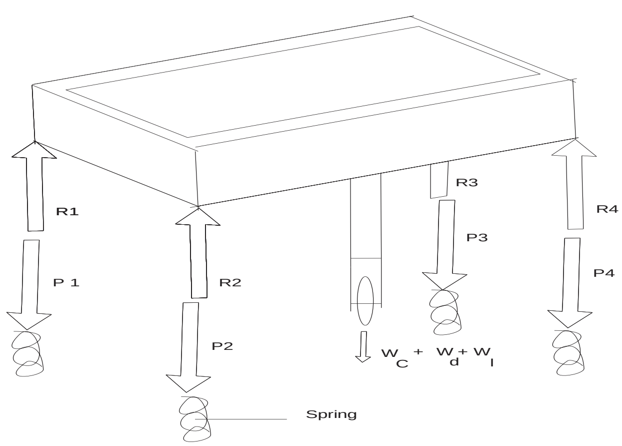

Figure 7 Freebody diagram of the vibrating chamber and the spring

$$+\uparrow \sum F_y = 0, \quad (148)$$

$$\text{Total upward force} - \text{Total downward force} = 0 \quad (149)$$

Total upward force = $R_1+R_2+R_3+R_4$ (150)

Since the springs are identical,

$R= R_1= R_2 =R_3 = R_4$ (151)

Total upward force $= R + R + R + R = 4R$ (152)

$R -$ the total reaction of all the four spring, N

$+\uparrow \sum F_x = 0,$ (153)

In y-direction, we have

$+\uparrow \sum F_y = 0,$ (154)

Total upward force – Total downward force $= 0$ (155)

$4R - W_C - W_d - W_l = 0$ (156)

$R = \frac{524.2337}{4} = 131.0584\ N$ (157)

The action force (P) acting on the spring due to the weight of the vibrating chamber, follower rod and follower roller is equal to the reaction (R) of the spring on the vibrating chamber with the follower rod and the follower roller. This indicates that:

$P_1= R_1 = 131.0584\ N$, $P_2 = R_2 = 131.0584\ N$, $P_3 = R_3= 131.0584\ N$, $P_4 = R_4= 131.0584\ N$

Since $R_1= R_2 =R_3 = R_4$ (158)

Therefore, $P = P_1= P_2 =P_3 = P_4 = 131.0584\ N$ (159)

The axial load acting on the spring at equilibrium that is before vibration was $131.0584\ N$. When force was acting at the centre of the circular spring and the coils of spring were almost parallel to each other, no bending moment would result at any section of the spring (no moment arm), except torsion and shear force.

This value of P would was used to deflection of the helical spring.

Deflection of the helical spring

The deflection of the helical spring after mounting the vibrating chamber on top of the springs was obtained as follows:

$k = \frac{P}{\delta}$ (160)

Where,

$k -$ the spring stiffness or the spring rate,

$P -$ The axial load acting on each spring at equilibrium that is before vibration, N

$\delta -$ the deflection of the spring as the axial load act on the spring, m

Taking the stiffness of the spring as 15, 000 N/m. The axial load acting on each spring at equilibrium is 131.0584 N. Therefore, the deflection of spring is:

$$\delta = \frac{P}{k} = \frac{131.0584}{15,000} = 0.008737\ m \text{ or } 8.7 \text{ mm} \quad (161)$$

Number of coils or turns of helical spring, n

The part of the coils which was in contact with the seat does not contribute to spring action and hence are termed as inactive (dead) coils. The turns which impart spring action were known as active turns. The two ends coils sit flat and are inactive (they do not deform under load) so the number of active coil is equal to the total number of coil minus 2.

$$N_a = N_t - 2 \quad (162)$$

The recommended range of active turn was $3 \leq N_a \leq 18$.

The active number of turn of coil of the spring was taken has 18.

$$N_t = N_a + 2 = 18 + 2 = 20 \quad (163)$$

The total number of turn of coil N_t of the spring selected and used for the project was 20.

Spring index

A spring index in the range of 6 to 12 was recommended for close tolerance and those subjected to cyclic loading. The value of stiffness will increase as the value of D increases. The spring index was taken as 7.

$$C = 7 \quad (164)$$

This value was used to determine the wire diameter of the spring.

Wire diameter of the helical spring

The springs were designed in order to withstand stress by ensuring that the maximum stress that was imposed on it did not exceed the allowable or permissible stress of the material in which the spring was made from. For a given wire diameter, a spring with smaller diameter will experience more difference of shear strain between outside surface and inside surface compared to its counterpart. Stress problems occur when the spring index is too low or too high. As per stress, deflection is inversely proportional to wire diameter of coil spring. A coil spring of higher diameter was used so as to reduce stress. According to the equations obtained from Wei *et al.* (2016); Bhatt *et al.* (2016) the wire diameter of the spring was calculated as shown below:

$$\frac{P\delta}{2} = \frac{T\theta}{2} = \frac{T}{2} \quad \left(\frac{TL}{GJ}\right) \tag{165}$$

$$T = \frac{PD_m}{2} \tag{166}$$

$$L = \pi D_m N_a \tag{167}$$

$$J = \frac{\pi d^4}{32} \tag{168}$$

$$\delta = \frac{2}{P} \quad \left(\frac{T^2 L}{2GJ}\right) \tag{169}$$

$$\delta = \frac{2}{P} \quad \frac{\left(\frac{PD_m}{2}\right)^2 (\pi D_m N_a)}{2G\left(\frac{\pi d^4}{32}\right)} \tag{170}$$

$$\delta = \left(\frac{8PD_m{}^2 N_a}{Gd^4}\right) \tag{171}$$

$$\delta = \left(\frac{8PC^3 N_a}{Gd}\right) \tag{172}$$

$$d = \left(\frac{8PC^3 N_a}{G\delta}\right) \tag{173}$$

Where,

G− Modulus of rigidity

d−Wire diameter, m

n− number of free coils

D− Mean coil diameter,

The modulus of rigidity, G of helical spring made from chromium vanadium steel is 80 GN/m^2. The axial load acting on each spring at equilibrium is 131.0584 N.

$$P = 131.0584 \text{ N}, \; C = 8, N_a = 18, \; \delta = 0.008737 \; m \text{ and } G = 80 \text{ KN/m}^2 \tag{174}$$

$$d = \left(\frac{8\times131.0584\times8^3\times18}{80\times10^9\times0.008737}\right) \tag{175}$$

$$d = \left(\frac{6473236.493}{698960000}\right) \tag{176}$$

$$d = 0.009261 \; m \text{ or } 9 \text{ mm} \tag{177}$$

The 8 mm wire diameter of the spring was available in the market which was closed to the designed value. The wire diameter selected and used was 8 mm.

Mean diameter of the coil of the spring, D_m

Mean coil diameter of the helical spring was given as:

$$D_m = Cd \tag{178}$$

Where,

$D_m -$ Mean diameter of the coil of the spring, mm

$d -$diameter of the spring wire, mm

$C -$Spring index

The spring index was taking as 7 and wire diameter of spring was 0.008 m or 8 mm. Therefore using the equation presented by Sataynarayana *et al.* (2020) the mean diameter of the coil of the spring was calculated as follows:

$$D_m = Cd = 7 \times 8 = 64\ mm \tag{179}$$

The 60 mm mean diameter of spring was available in the market which closed to the designed value. The selected spring for the project has a mean diameter of 60 mm.

Outer diameter of the coil of the spring, $\boldsymbol{D_o}$

The outer diameter of the coil of the spring was calculated as follow:

$$D_o = D_m + d \tag{180}$$

Where,

$D_o -$ the outer diameter of the coil of the spring, mm

$D_m -$ Mean diameter of the coil of the spring, mm

$d -$diameter of the spring wire, mm

The Mean diameter of the coil of the spring is 64 mm and diameter of the spring wire is 8 mm.

$$D_o = D_m + d = 64 + 8 = 72\ mm \tag{181}$$

The 68 mm outer diameter of spring was available in the market which was closed to the designed value. The selected spring for the project has an outer diameter of 68 mm.

Inner diameter of the coil of the spring, $\boldsymbol{D_o}$

The inner diameter of the coil of the spring was evaluated using:

$$D_i = D_m - d \tag{182}$$

Where,

$D_i -$ the inner diameter of the coil of the spring, mm

$D_m -$ Mean diameter of the coil of the spring, mm

$d -$ Diameter of the spring wire, mm

$$D_i = D_m - d = 64 - 8 = 56\ mm \tag{183}$$

The 52 mm inner diameter of spring was available in the market which was closed to the designed value. The selected spring for the project has an inner diameter of 52 mm.

Stresses in the helical spring wire

Stress analysis was carried out to ensure that the spring element will not fail sue to stress levels exceeding the allowable values. As the spring element is subjected axial load due to the weight of the vibrating chamber, it experiences a torsional shear stress and a transverse shear stress. In addition, there is an additional stress effect due to curvature.

For compressive load on the spring, maximum shear stress always occurs at the inner side of the spring. Failure of the spring, in the form of crack, is always initiated from the inner radius of the spring where the shearing stress maximum. The maximum shearing stress is located at the inner side of the curved wire. The radius of the spring was given by D/2.

Where,

D was the mean diameter of the spring.

The torque acting on the spring was

$$T = F \times \frac{D_m}{2} \tag{184}$$

If d was the diameter of the coil wire and I_p was polar moment of inertia, then

$$I_p = \frac{\pi d^4}{32} \tag{185}$$

The shear stress in the spring wire due to torsion was given as

$$\tau_T = \frac{T_r}{I_p} = \frac{F \times \frac{D_m}{2} \times \frac{d}{2}}{\frac{\pi d^4}{32}} = \frac{8FD_m}{\pi d^3} \tag{186}$$

Average shear stress in the spring wire due to force F was

$$\tau_F = \frac{F}{\frac{\pi d^2}{4}} = \frac{4F}{\pi d^2} \tag{187}$$

Therefore, maximum shear stress of the spring wire was

$$\tau_T + \tau_F = \frac{8FD_m}{\pi d^3} + \frac{4F}{\pi d^2} \tag{188}$$

$$\tau_{max} = \frac{8FD_m}{\pi d^3}\left(1 + \frac{1}{\frac{2D_m}{d}}\right) \tag{189}$$

$$\tau_{max} = \frac{8FD_m}{\pi d^3}\left(1 + \frac{1}{2C}\right) \tag{190}$$

Where,

$C = \frac{D_m}{d}$, is called the spring index (191)

$$\tau_{max} = K_s \frac{8FD_m}{\pi d^3} \tag{192}$$

Where,

$$K_s = \left(1 + \frac{1}{2C}\right) \tag{193}$$

$K_s -$ the shear stress correction factor

For a given wire diameter, a spring with smaller diameter will experience more difference of shear strain between outside surface and inside surface compared to its counterpart. The above phenomenon is termed as curvature effect. According to Vukelic *et al.* (2017) to take care of the curvature effect, the earlier equation for maximum shear stress in the spring wire is modified as,

$$\tau_{max} = K_w \frac{8PD_m}{\pi d^3} \tag{194}$$

Where, K_w is Wahl correction factor, which takes care of both curvature effect and shear stress correction factor and Ambhore *et al.* (2016); Tan *et al.* (2020) expressed K_w as,

$$K_w = \frac{4C-1}{4C-4} + \frac{0.615}{C} \tag{195}$$

This is for more conservative design. Failure occurs when the maximum shear stress at a point exceeds the maximum allowable shear stress for the material. The allowable shear stress of helical spring made from chrome-vanadium steel, oil tempered hot wound and heat treated forming of diameter 4.625 to 8 mm is 294 MPa for severe service. The higher the wire diameter of spring the lesser the allowable stress. The spring index was taken as 7.

Therefore, the stress correction factor is:

$$K_w = \frac{4C-1}{4C-4} + \frac{0.615}{C} = \frac{(4\times7)-1}{4(7)-4} + \frac{0.615}{7} = 1.21286 \tag{196}$$

$$\tau_{max} = K_w \frac{8PD_m}{\pi d^3} \tag{197}$$

$K_w = 1.21286, P = 131.0584\ N, D_m = 64\ mm\ or\ 0.0064\ m\ and\ d = 0.008\ m\ or\ 8\ mm$

$$\tau_{max} = 1.21286 \times \frac{8\times131.0584\times0.0064}{\pi\,(0.008)^3} = 5.0597\ MN/m^2 \tag{198}$$

Since $\tau_{max}(5.0597\ MN/m^2)$ is less than (within) the allowable or permissible shear stress 294 MN/m^2

The design was acceptable.

Free length of spring

A helical compression spring that is too long compared to the mean coil diameter acts as a flexible column may buckle at comparatively low axial force. Spring which cannot be designed buckle-proof must be guided in a sleeve over an arbor. This is undesirable because the friction between the spring and the guide may damage the spring in the long run.

If

$\frac{Free\ length}{Mean\ coil\ diameter} \leq 2.6$ (Guid not necessary) (199)

$\frac{Free\ length}{Mean\ coil\ diameter} \geq 2.6$ (Guid required) (200)

Free length $l_o \geq (N_t)d + y + a$ (201)

Where,

l_o – free length, m

$i - Number\ of\ the\ active\ turns\ of\ coils$

n$-number\ of\ additional\ coil,\ n = 2$

y –maximum deflection, m

a$-$ clearance which is 25 % of maximum deflection

Assuming squared and ground end

$N_t = N_a + 2$ (202)

$N_a = 18$ (203)

$N_t = 18 + 2 = 20$ (204)

Maximum deflection = y (205)

$y = y_{chamber} + y_{vibration}$ (206)

Where,

$y_{chamber} -$ the deflection due to the loaded vibration chamber on the spring, m

$y_{vibration}$ $-$the deflection of the spring due to the vibration exciter, m

$y_{chamber} = \delta = 0.0087\ m\ and\ y_{vibration}$ = maximum amplitude of vibration = 20 mm or 0.02 m

$y = y_{chamber} + y_{vibration}$ (207)

$y = 0.0087 + 0.02 = 0.0287\ m$ (208)

$a = 25\,\%\,of\;y = 25\% \;\times\; 0.0287 = 0.007175$ m (209)

Free length $l_o \;\geq (N_t)d + y + a$ (210)

$N_t \;= 20, d = 8\;mm\;or\;0.008\;m\;y = 0.0287\;m\;and\;a = 0.007175\;m$

Free length $l_o \;\geq (20) \times 0.008 + 0.0287 + 0.007175$ (211)

$l_o \;\geq 0.1959\;m$ (212)

The free length = 0.20 m (213)

The available spring length found in the market was 0.15 m. Buckling was check for using this length value.

To check for buckling

$$\frac{Free\;length}{Mean\;coil\;diameter}$$

Free length = l_o = 0.15 m and Mean coil diameter used for the project was = 60 mm or 0.060 m

$$\frac{0.15}{0.060}$$

$2.5 \leq 2.6$ (214)

Since the ratio of the free length to the mean coil diameter was less than 2.6, so the spring did not need any guide.

Solid length of spring

The solid length of a spring was the product of total number of the coils and the diameter of the wire. So, $L_s = N_t d$ = 20 × 0.008 = 0.16 m or 16 mm

Since 150 mm was the free length of spring selected, therefore the solid length of the spring selected was

Solid length = $(20) \times 0.008 - 0.0287 - 0.007175 = \;0.1241$ m or 124.1 mm (215)

The solid length of the spring used for the project was 124.1 mm

Pitch of the spring

Pitch of the spring is the number of coils per unit of the length of the spring. Pitch of the spring used for the project was determined from:

$p = \frac{l_o - 2d}{N_a}$ (216)

$l_o = 0.15\;m, d = 0.008\;m\;or\;8\;mm\;and\;N_a \;= 20$

$p = \frac{0.15 - 2 \times 0.008}{18} = 0.007444\;m\;or\;7.44\;mm$ (217)

Stability (Buckling) of the spring

Buckling is an instability that is normally shown up when a long or too slender spring is applied with compressive type of load. Bucking may occur in compression springs if the free length is over four times the mean diameter unless the spring is properly guided. At this condition the spring behaves like a column which may fail by buckling at a comparatively low load.

Free length selected = l_o $= 0.15$ m and Mean coil diameter selected= D_m =60 mm or 0.060 m

$$\frac{Free\ length}{Mean\ coil\ diameter} = \frac{0.15}{0.060} \tag{218}$$

$$\frac{Free\ length}{Mean\ coil\ diameter} = 2.5 < 4 \tag{219}$$

Since the ratio of the free length to mean coil diameter of the spring was less than four the design was safe from buckling. The Table 7 indicates the design specification of the helical compression spring.

Table 7 Design specification of the spring

S/N	Spring parameters	Specification
1	Material selection	Chrome Vanadium steel
2	Deflection of the helical spring, δ	8.7 mm
3	active number of turn of coil of the spring, N_a	18
4	total number of turn of coil of the spring, N_t	20
5	spring index, C	7
6	Wire diameter of spring, d	8 mm
7	Mean diameter of spring, D_m	60 mm
8	outer diameter of the coil of the spring, D_o	68 mm
9	the inner diameter of the coil of the spring, D_i	52 mm
10	Free length of the spring, l_o	150 mm
11	Solid length of the spring, L_s	124.1 mm
12	Pitch of the spring, p	7.44 mm

2.2.7 Design of the Speed of electric motor

The selection of the frequency range for the yam vibration was based on the possible and achievable frequency range reported for mechanical vibrator. Nitinkumar *et al.* (2014) reported that the frequency range of mechanical vibrator (using eccentric and connecting link, scotch yoke, cam and follower or rotating unbalance mass mechanism) falls between 0 – 200 Hz. The maximum attainable frequency (200 Hz) was divided into three categories (low, medium and very high frequency). Where the low frequency has frequency range of (1 – 5) Hz and the medium has frequency range of (60 – 100 Hz) and the high frequency has frequency range of (150 – 200 Hz)

From one level of frequency to another gap was provided to avoid overlapping of result and to allow distinct analysis of level over the other. The Frequencies of vibration required for the vibration of the yam tuber were 1 – 5 Hz, 60 – 100 Hz and 150 – 200 Hz. The frequency of vibration of the vibrating chamber depends on the speed of the electric motor. According Prayitnoadi *et al.* (2019) the relationship between the frequencies of vibration of the vibrating chamber and the speed of the electric motor is shown below:

$$f_{vibration} = \frac{\omega}{60} \qquad (220)$$

Where,

$f_{vibration}$ = frequency of vibration of the vibrating chamber in rev/sec (Hz)

ω = angular velocity of the electric motor in rpm (revolution per minute)

The maximum angular velocity of the electric motor required for the low (1 – 5 Hz), medium (60 – 100 Hz) and (150 – 200 Hz) were 300 rpm, 6000 rpm and 12, 000 rpm. To achieve this, variable speed electric motor that had the ability to generate a speed more than 12, 000 rpm was selected and used for the project. The Table 8 shows the required angular velocity of the electric motor for the vibrating system.

2.3 Selection of the frequency of the mechanical yam vibrator

The selection of the frequency range for the yam vibration was based on the possible and achievable frequency range reported for mechanical vibrator. Nitinkumar *et al.* (2014) reported that the frequency range of mechanical vibrator (using eccentric and connecting link, scotch yoke, cam and follower or rotating unbalance mass mechanism) falls between 0 – 200 Hz. The maximum attainable frequency (200 Hz) was divided into three categories (low, medium and very high frequency). Where the low frequency has frequency range of (1 – 5) Hz and the medium has frequency range of (60 – 100 Hz) and the high frequency has frequency range of (150 – 200 Hz). From one level of frequency to another gap was provided to avoid overlapping of result and to allow distinct analysis of level over the other. The Frequencies of vibration required for the vibration of the yam tuber were 1 – 5 Hz, 60 – 100 Hz and 150 – 200 Hz.

Plate 1 View of the mechanical yam vibrator during construction

Plate 6 The view of the developed mechanical yam vibrator with adjustable frequency and amplitude

2.4 Selection of the amplitude of the vibration exciter

The selection of the amplitude range for the yam vibration was based on the possible and achievable amplitude range reported for mechanical vibrator. Nitinkumar *et al.* (2014) reported that maximum displacement (amplitude) of mechanical vibrator (using eccentric and connecting link, scotch yoke, cam and follower or rotating unbalance mass mechanism) achievable is 25 mm. The maximum amplitude was staged at 20 mm and was divided in three categories (low, medium and high levels). The level of the amplitude was increased using a quadratic progression in order to cover the range of the achievable amplitude reported; where the low, medium and high amplitudes were 5 mm, 10 mm and 20 mm.

2.5 Preliminary Test on the Developed Mechanical Yam Vibrator

Preliminary test was conducted on the developed mechanical yam vibrator to ascertain its workability. A vibrometer obtained from the mechanical department was used to determine the variation of the displacement of developed mechanical yam vibrator at different combination of levels of amplitude and frequency.

Three sets of cams size developed were used to have three set of maximum displacements at three different frequencies. The constructed sets of maximum displacement of the cam used were 5 mm, 10 mm and 20 mm while each set of cam was operated with three different frequencies which were low (1 – 5 Hz), medium (60 – 100 Hz) and high (150 – 200 Hz). For each treatment of vibration the lobe of the vibrometer was placed inside the mechanical yam vibrator while the variation of displacement was monitored and recorded.

Table 8 The required angular velocity of the electric motor for the vibrating system

Series number (Levels)	Required Frequency of vibration of the yam tubers (Hz)	Maximum required angular velocity of the electric motor for each level (rpm)
1	1 – 5	300
2	60 – 100	6, 000
3	150 – 200	12, 000

3.0 Results and Discussion

Variation of the displacement of the vibration of the mechanical yam vibrator

Figures 13 – 21 show the pattern of variations of the displacement of the vibration of the mechanical yam vibrator with time at different levels of frequency and amplitude which were recorded from 13/01/2020 to 14/01/2020. The Figure proved that there were variations in the displacement of the vibration of the mechanical yam vibrator developed. The purpose of evaluating the vibration parameter of the mechanical vibrator was to ascertain it workability before using it for the vigorous work and to prevent fail of the developed machine during the vibration session of the yam tuber to be used for the experimental study. The plots also indicated that at combined different levels of the frequency and amplitude the pattern of vibration they were not the same. The variations in pattern were as a result of the different cam profile used for the different level of amplitude and the variation of the levels of frequency. From the preliminary test the maximum displacement of the developed mechanical yam vibrator using a cam size of 5 mm, 10 and 20 mm are 4.66 mm, 9.09 mm and 17.30 mm respectively.

Conclusion

This developed a mechanical yam vibrator having adjustable frequencies and amplitudes at Federal University of Abeokuta, Ogun State, Nigeria with vibrating chamber of capacity size of 670 mm × 570 mm × 180 mm which can contain four tubers of yam at a time. The electric motor that powered the mechanical yam vibrator operates at angular velocity ranging from 0 – 12, 000 revs/second. The preliminary test conducted indicates that the maximum displacement of the developed mechanical yam vibrator using a cam size of 5 mm, 10 and 20 mm are 4.66 mm, 9.09 mm and 17.30 mm respectively at different levels of frequencies (low frequency (1 – 5 Hz), medium frequency (60 – 100 Hz) and high frequency (150 – 200 Hz). This proved that the developed mechanical yam vibration provide variation in displacement and frequency which would help in generating different levels of displacement and frequency for the yam tubers to be vibrated.

1.
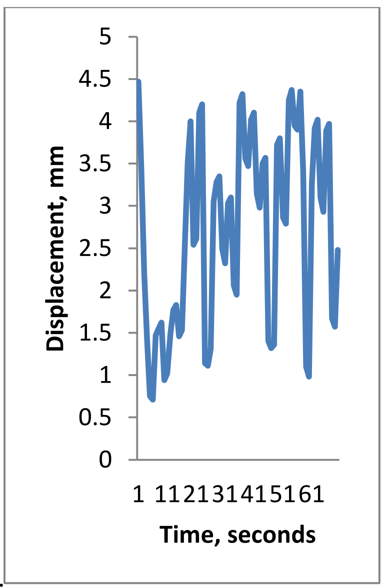

2.
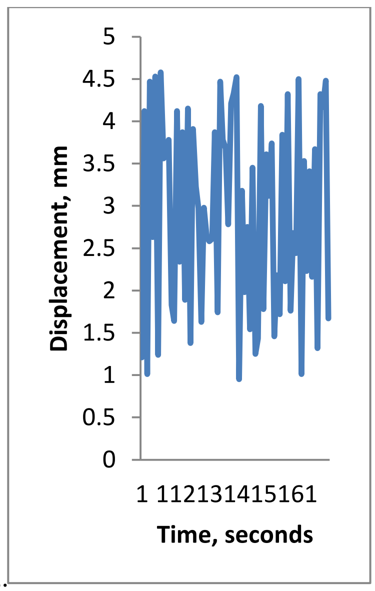

3.
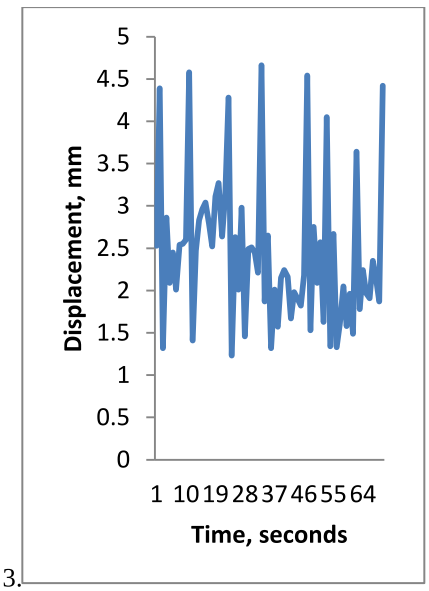

Figure 13 Displacement time of the mechanical vibration at low frequency (1 – 5 Hz) and low amplitude (5 mm)

Figure 14. Displacement time of the mechanical vibration at medium frequency (60 – 100 Hz) and low amplitude (5 mm)

Figure 15. Displacement time of the mechanical vibration at high frequency (150 – 200 Hz) and low amplitude (5 mm)

16. 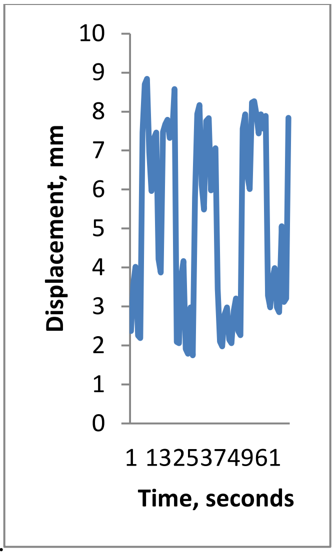

17. 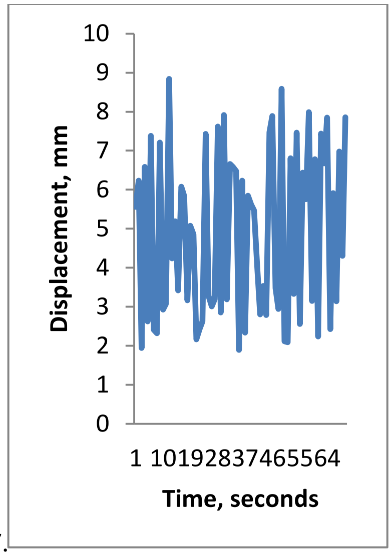

18. 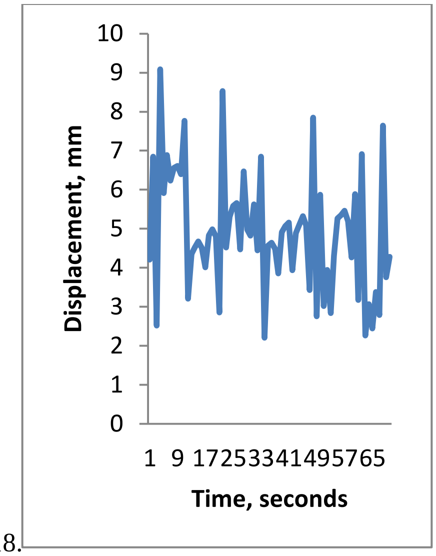

Figure 16. Displacement time of the vibration at low frequency (1 – 5 Hz) and medium amplitude (10 mm)

Figure 17. Displacement time of the mechanical vibration at medium frequency (60 – 100 Hz) and medium amplitude (10 mm)

Figure 18. Displacement time of the mechanical vibration at high frequency (150 – 200 Hz) and medium amplitude (10 mm)

7. 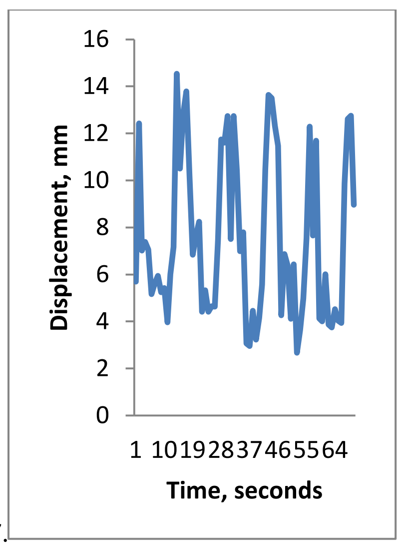

8. 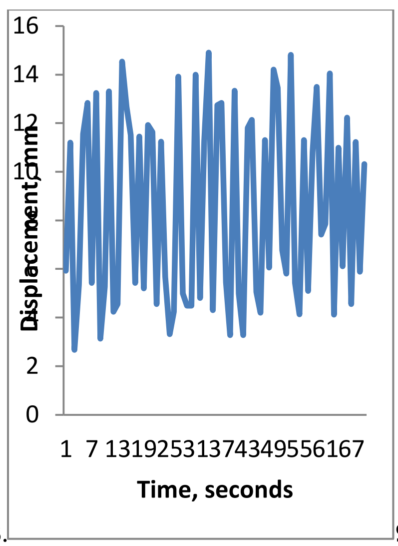

9. 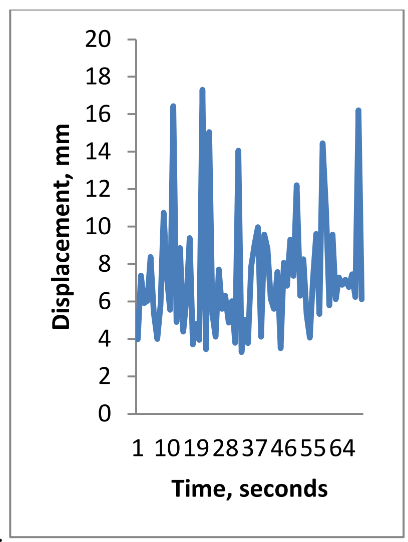

Figure 19. Displacement time of the mechanical vibration at low frequency (1 – 5 Hz) and high amplitude (20 mm)

Figure 20. Displacement time of the vibration at medium frequency (1 – 5 Hz) and high amplitude (20 mm)

Figure 21. Displacement time of the mechanical vibration at high frequency (1 – 5 Hz) and high amplitude (20 mm)

References

Abewoy D. (2021). Review on Postharvest Handling Practices of Root and Tuber Crops. International Journal of Plant Breeding and Crop Science *8 (1): 992 – 1000.*

Akusu O.M., Oyejide J.O., Udumebraye J.E. (2018). Design and C onstruction of Dried Cassava Pellets Grinding Machine. American Journal of Engineering Research *7 (3): 46 – 55.*

Ambhore P.J., Bhore H.G., Raut R., Chaudhari D. (2016). Stress Analysis Two Wheeler Helical Coil Spring for Different Material. Journal of Mechanical and Civil Engineering *13 (3): 46 – 50.*

Anyakoha M.W. (2016). New School Physics for Senior Secondary School. Africana First Publisher Plc, Enugu, Nigeria 532 pg.

Bhatt A., Devani A., Zalavadiya P. (2016). Design Analysis of Helical Spring of Suspension System. International Journal of Engineering Development and Research *4 (3): 1 – 13.*

Brian W., Brandon D. (2010). Design of a Vibration Exciter Device. Honor Theses, Mechanical Engineering Senior Design Project, Western Michigan University, 1903 W Michigan Ave, Kalamazoo, MI 49008, USA 97 pg.

Cheema M. U.A. (2010). Dormancy and Sprout Control in Root and Tuber Crops. Thesis for the Degree of Doctor of Philosophy. Natural Resources Institute, University of Greenwich, UK 276 pg.

Childs P.R.N (2013). Mechanical Design Engineering Handbook. Technology and Engineering 856 pg.

Ei T.T., Latt A.K., Win H.H. (2019). Structural Analysis of Shafts and Performance Test of Paddy Thresher *3 (3): 1 – 7.*

Ekeocha R.J.O. (2018). Vibration of Systems. Journal of Mechanical Engineering Research *10 (1): 1 – 6.*

Engineering ToolBox (2008). Engineering Material. Engineering ToolBox online 1 pg.

Kevers C., Ovono P.O., Dommes J. (2010). Effects of Storage Conditions on Sprouting of Microtubers of Yam (*Dioscorea cayenensis – D. rotundata*). Comptes Rendus Biologies *333: 28 – 34.*

Khurmi R.S., Gupta J.K. (2005). A textbook of Machine Design. S. Chand Publishing 1230 pg.

Lamancusa J.S. (2002). Vibration Isolation. Noise Control *12: 1 – 14.*

Manikumar R., Rajasekhar S., Reddy N.K.Y., Harshavardha V. (2019). Torsional Behaviour of a Propeller Shaft Material and its Optimization *6 (4): 4871 – 4878.*

Nitinkumar A., Ruiwale V.V., Nimbalkar S., Rao P. (2014). Design and Testing of Unbalanced Mass Mechanical Vibration Exciter. International Journal of Research in Engineering and Technology *3 (8): 107 – 112.*

Pawar A., Vajre S., Patil S., Badade A., Sasane K. (2016). Design and Fabrication of Mechanical Vibration Exciter. International Journal of Mechanical Engineering and Technology *7(6): 58 – 75.*

Pederson N.L. (2010). Stress Concentrations in Keyways and Optimization of Keyway Design. The Journal of Strain Analysis for Engineering Design *45: 593 – 604.*

Prayitnoadi R.P., Hudatwi F.R.M., Nurhadi M.U., Febrianto A., Roliana N. (2019). Analysis of Sea Wave Power Plant Design in Bangha Island Indonesia. IOP Conference Series: Material Science and Engineering *694: 1 – 6.*

Okeke P.N. (2016). New School Physics for Senior Secondary Schools. Macmillan Education, London 156 pg.

Onyenwoke C.A., Simonyan K.J. (2014). Cassava Post – Harvest Processing and Storage in Nigeria: A review. African Journal of Agricultural Research *9 (53): 3853 – 3863.*

Sataynarayana K., Ugesh T., Gowri B., Ganesh D.S.A., Bharath K. (2020). Design and Static Analysis on a Helical Spring for Two Wheeler. A Journal of Composition Theory *8 (3): 1439 – 1449.*

Savinkin V.V., Kolisnichenko S.N., Sandu A.V., Ivanova O.V., Vizureanu P., Zhumekenova Z.Z. (2021). Investigation of the Strength Parameters of Drilling Pumps during the Formation of Contact Stresses in Gears. Applied Sciences *11 (7076): 1 – 22.*

Socha B.J., Bednarz E.T., Zhu W. (2020). A Combined Loading Transducer for Calculating the Bending Moment and Torque in a Slender Circular Beam using the Minimum Numbers of Strain Gauges, Strain Grids, and Measurement Channels. International Journal of Distributed Sensor Networks *16 (6): 1 – 10.*

Tan P.S., Farid A.A., Karimzaadeh A., Koloor S.S.R. (2020). Investigation on the Curvature Correction Factor of Extension Spring. Materials *13: 4199 – 4214.*

Wei D., Fyrillas M., Otemissov A., Bekishev R. (2016). Optimal Design of Helical Springs of Power Materials. Nazarbayev University, Kabanbay Batyr Ave., Astana, Kazakhstan, Central Asia 12 pg.

Wickham L.D. (2019). Successful Manipulation of the Growth Cycle of Yam (*Dioscorea spp.*) for Year – Round Production for Food Security and Climate Change. Trop. Agric. *96: 27 – 39.*

Vukelic G., Brcic M., Pastoric D. (2017). Experimental and Numerical Analysis of a Helical Spring Failure. International Conference on Computional Plasticity, Fundamentals and Applications pg 545 – 555.